Skeletal muscles of sedentary and physically active aged people have distinctive genic extrachromosomal circular DNA profiles

Supplementary Material

Daniela Gerovska[1*] and Marcos J. Araúzo-Bravo[1,2,3,4,5*]

[1] Computational Biology and Systems Biomedicine, Biodonostia Health Research Institute, Calle Doctor Begiristain s/n, 20014, San Sebastian, Spain

[2] Basque Foundation for Science, IKERBASQUE, Calle María Díaz Harokoa 3, 48013, Bilbao, Spain

[3] CIBER of Frailty and Healthy Aging (CIBERfes), Madrid, Spain

[4] Max Planck Institute for Molecular Biomedicine, Computational Biology and Bioinformatics, Röntgenstr. 20, 48149, Münster, Germany

[5] Department of Cell Biology and Histology, Faculty of Medicine and Nursing, University of Basque Country (UPV/EHU), 48940 Leioa, Spain

* Corresponding authors: Daniela Gerovska: daniela.gerovska@biodonostia.org, Marcos J. Araúzo-Bravo: mararabra@yahoo.co.uk

Daniela Gerovska ORCID: orcid.org/0000-0003-0671-4277

Marcos J. Araúzo-Bravo ORCID: orcid.org/0000-0002-3264-464X

Supplementary Tables

Table S1. Up-DPpGC-associated genes for the TS group and their function in SkM.

Gene	Function
AGBL4 (CCP4) AGBL carboxypeptidase 4	Obesity/BMI-associated locus with expression enrichment in the brain regions insula and substantia nigra, involved in addiction and reward (Ndiaye *et al.*, 2020); member of CCP enzyme family modifying MLCK (Rogowski *et al.*, 2010), with the smooth muscle smMLCK isoform specifically required to regulate smooth muscle contractility (Chen *et al.*, 2013).
RNF213 (mysterin) ring finger protein 213	Role in insulin-regulating pathways (Sarkar *et al.*, 2021); necessary for SkM myogenesis (Kotani *et al.*, 2015).
DNAH7 dynein axonemal heavy chain 7	Adipogenesis-associated gene (Söhle *et al.*, 2012).
MED13 mediator complex subunit 13	Role in governance of glucose metabolism and control of hepatic lipid accumulation by SkM (Amoasii *et al.*, 2016).
WWTR1 (TAZ) WW domain containing transcription regulator 1	Downstream effector in the Hippo pathway, plays key role in myoblast proliferation and enhances myogenic differentiation (Sun et al., 2017); Myoblast proliferation and differentiation is altered in aging, associated with low physical activity, which may alter YAP/TAZ levels in myoblasts, cause stiff extracellular matrix and induce further fibrosis through YAP/TAZ (Setiawan *et al.*, 2021).
CTD-2337A12.1 uncharacterized LOC101929710	rs6232 associated with a higher risk of obesity and insulin resistance (https://selfdecode.com/app/snp/rs6232/).
ADCY3 adenylate cyclase 3	ADCY3 variants are risk of obesity and T2D (Grarup *et al*., 2018).
HECW1 HECT, C2 and WW domain containing E3 ubiquitin protein ligase 1	Identified in muscle-invasive transitional cell carcinoma (Pan *et al*., 2016).
DNAH17 dynein axonemal heavy chain 17	Involved in fatty tissue biology, KD causes reduced neutral lipid accumulation (Söhle *et al.*, 2012).
SLC6A11 solute carrier family 6 member 11	Genetic perturbation of SLC16A11 induces changes in fatty acid and lipid metabolism associated with increased T2D risk (Rusu *et al.*, 2017).
...	**Upper row genes (10) in rank order; Lower row genes in alphabetic order**
ATP1A3 ATPase Na+/K+ transporting subunit alpha 3	Transmembrane ion-pump maintaining the electrochemical gradients of Na and K ions across the plasma membrane, important for electrical excitability of nerve and muscle.
BACE1 beta-secretase 1	Sustain muscle spindles and maintain motor coordination (Cheret *et al.*, 2013).
COL24A1 collagen type XXIV alpha 1 chain	Increased in insulin-resistant SkM and adipose tissue (Weng *et al.*, 2020).
NEK11 NIMA related kinase 11	Linked with DNA replication and response to genotoxic stress, central role in the G2/M checkpoint and the DNA damage response (Peres de Oliveira *et al.*, 2020).
NMT1 N-myristoyltransferase 1	Overexpressed and hypermethylated in visceral adipose tissue of severely obese individuals with Metabolic Syndrome; SNPs associated with altered plasma lipid levels, increased inflammation markers and blood pressure among severely obese patients (Bégin *et al.*, 2015).
SLC17A7 (*VGLUT1*) solute carrier family 17 member 7	Associated with the membranes of synaptic vesicles and functions in glutamate transport.
SYN2 synapsin II	Marker protein of synaptic vesicles filling the nerve terminal of neurons (Thiel, 1993).
UBE2D2 ubiquitin conjugating enzyme E2 D2	Role in atrophying SkM (Polge *et al*., 2015)

Table S2. Up-DPpGC-associated genes for the TA group and their function in SkM.

Gene	Function
ZBTB7C zinc finger and BTB domain containing 7C	Proto-oncoprotein, controls cell cycle and glucose, glutamate, and lipid metabolism; KO or KD of *Zbtb7c* decreases adipose tissue mass in aging mice (Choi *et al.*, 2021).
ENSG00000266893	Long intervening noncoding RNA
TBCD tubulin folding cofactor D	Significantly hypermethylated in aged muscle tissue (Zykovich *et al.*, 2014)
ITPR2 inositol 1,4,5-trisphosphate receptor type 2	Necessary for mitochondrial calcium uptake, KD associated to senescence escape, indicating the role of mitochondrial calcium accumulation in senescence induction (Wiel *et al.*, 2014); promotes cellular senescence and aging (Ziegler *et al.*, 2021)
DDX11-AS1 DEAD/H-box helicase 11 Antisense RNA 1	Long non-coding RNA; DDX11 involved in DNA replication and sister chromatid cohesion, possible role in DNA repair (Bharti *et al.*, 2014).
AACSP1 acetoacetyl-CoA synthetase pseudogene 1	Associated with cardiorespiratory fitness and endurance performance (Zhao *et al.*, 2020)
MCTP1 *multiple C2 and transmembrane domain containing 1*	Promotes lipid droplet biogenesis (Joshi *et al.*, 2021); SNP associated with physical activity (Kim *et al.*, 2014)
...	**Upper row genes in rank order; Lower row genes in alphabetic order**
AACSP1 acetoacetyl-CoA synthetase pseudogene 1	rs12518860 associated with cardiorespiratory endurance (Zhao *et al.*, 2020)
ADAM10 ADAM metallopeptidase domain 10	Indispensable for maintenance of the muscle satellite cell pool (Mizuno *et al.*, 2019)
CDCP1 (*CD318*) CUB domain containing protein 1	Expressed in satellite cells (Uezumi *et al.*, 2016); potential to preserve and recover SkM mass and function in cachexia, sarcopenia, and neuromuscular diseases.
CDKAL1 CDK5 regulatory subunit associated protein 1 like 1	T2D susceptibility gene; regulates mitochondrial function in adipose tissue, mRNA levels reduced in adipose tissue of obese mice (Palmer *et al.*, 2017).
KYAT1 (*KAT1*) kynurenine aminotransferase 1	Catalyzes the production of kynurenic acid which activates GPR35/AMPK and SIRT6 pathways and reduces inflammation and insulin resistance in SkM (Jung *et al.*, 2020).
MFN2 mitofusin 2	Adult SkM deletion impedes exercise performance and training capacity (Bell *et al.*, 1985).
NEB nebulin	Regulates thin filament length, contractility, and Z-disk structure *in vivo*. Myopathic changes in the nebulin KO model include depressed contractility, loss of myopalladin from the Z-disk, and dysregulation of genes involved in calcium homeostasis and glycogen metabolism (Witt *et al.*, 2006)
PPP2R5E protein phosphatase 2 regulatory subunit B'epsilon	Implicated in the negative control of cell growth and division. Gene affected by exercise (Radom-Aizik *et al.*, 2009).
ROR2 receptor tyrosine kinase like orphan receptor 2	Roles in morphogenesis and formation of the musculoskeletal system during embryonic development and its regeneration and maintenance in adults (Kamizaki *et al.*, 2021).
RPS6KA1 ribosomal protein S6 kinase A1	Influences healthy mammalian life-span; its therapeutic manipulation mimics caloric restriction and protect against diseases of aging (Selman *et al.*, 2009)
STRBP spermatid perinuclear RNA binding protein	Highly expressed in testis and brain; negatively correlated with age and aging (Li *et al.*, 2019).
TNIP1 TNFAIP3 interacting protein 1	Repressor of inflammatory signaling and factor in autoimmune diseases (Shamilov *et al.*, 2018).
TSHZ3-AS1 TSHZ3 antisense RNA 1	Expressed in quiescent satellite cells of adult mouse SkM; regulates SkM differentiation (Faralli *et al.*, 2011).

Table S3. Functional enrichment analysis of DPpGCs overrepresented in TS based on the DisGeNET annotation. Number of genes in the signal set 158. Number of genes in the background set 10771.

Count	*p*-value	DisGeNET	Genes
11/139	$2.050e^{-4}$	Smoking Behaviors	*ASIC2, CDH13, CHRNB4, DYTN, HECW1, MYO9B, PBRM1, PTPRD, RSPO3, RUNX1, SNX25*
4/19	$4.033e^{-4}$	Abnormal coordination	*ATP1A3, ATXN10, CACNA2D2, LMBRD1*
5/35	$5.908e^{-4}$	Ataxia, Appendicular	*ATP1A3, ATXN10, CACNA2D2, CYP7B1, FGF12*
15/267	$8.168e^{-4}$	Waist-Hip Ratio	*AGBL4, ASTN2, CDH13, COL24A1, DLG2 ,DNAH17, EPHB1, MYO9B, PBRM1, RNF157, RSPO3, RUNX1, SPATA5, WDR35, ZFAT*
4/26	$1.413e^{-3}$	Apathy	*AR, ATXN10, LRRK2, MSN*
13/228	$1.462e^{-3}$	Diastolic blood pressure	*ADCY3, ASTN2, CACNA2D2, CDH13, DNAH7 ,EBF1 ,LINC01762, LIPC LRRC8C, MYO9B, NXN, PTPRD, UBE2D3*
4/27	$1.636e^{-3}$	Thymic Carcinoma	*AR, ERCC1, PBRM1, SORBS1*
4/28	$1.882e^{-3}$	Widely spaced teeth	*ATP1A3,SPATA5, WDR35, ZSWIM6*
4/29	$2.153e^{-3}$	Anhedonia	*ATP1A3, CDYL, CHRNB4, SLC17A7*
4/29	$2.153e^{-3}$	Motor symptoms	*AR, ATP1A3, LRRK2, SLC17A7*
5/48	$2.554e^{-3}$	Complex partial seizures	*ATXN10, CHRNB4, ERCC1 ,SLC17A7, SYN2*
4/32	$3.127e^{-3}$	Cerebellar Diseases	*ATP1A3, CYP7B1, FLNC, SLC17A7*
6/71	$3.206e^{-3}$	Response to bronchodilator	*CDH13, CHRNB4,DLG2, FGF12, PPM1L, PTPRD*
5/52	$3.647e^{-3}$	Eversion of lower lip	*ERCC1, PHGDH, QRICH1, WDR35, ZSWIM6*
6/74	$3.949e^{-3}$	Epileptic encephalopathy	*ATP1A3 ,CACNA2D2, FGF12 ,PHGDH, SPATA5, ST3GAL3*
5/55	$4.662e^{-3}$	Dystonia Disorders	*ATP1A3 ,DST, GNAL ,LRRK2, RGS9*
4/39	$6.490e^{-3}$	Hip circumference	*ADCY3, EBF1, RSPO3, ZFAT*
4/39	$6.490e^{-3}$	Alopecia, Male Pattern	*AR, EBF1, RUNX1 ,STS*
4/40	$7.112e^{-3}$	Tachycardia, Ventricular	*FGF12, FLNC, RYR1, SEC1P*
7/112	$8.750e^{-3}$	Neurofibromatosis 1	*AR, ASIC2 ,EPHB1 ,NFIA ,RNF213,RUNX1 ,RYR1*
7/114	$9.606e^{-3}$	Hyporeflexia	*AR, ATXN10, FGF12 ,FLNC, QRICH1, RYR1, ZSWIM6*
4/44	$9.992e^{-3}$	Epileptic drop attack	*CHRNB4, PHGDH, SLC17A7 SYN2*
7/119	$1.201e^{-2}$	Dyskinetic syndrome	*ATP1A3, ATXN10, FGF12, LRRK2, RGS9, SPATA5, ST3GAL3*
14/332	$1.428e^{-2}$	Adolescent idiopathic scoliosis	*AR, ASIC2, ASTN2, ATXN10, CDH13, COL24A1, DLG2, GALNT16, LINC02119, LIPC, PTPRD, SORCS2, STX18, SYN2*
4/49	$1.454e^{-2}$	X- linked recessive	*ABCA4, AR, MSN, STS*
4/50	$1.559e^{-2}$	Aplastic Anemia	*AR, MSN, RUNX1, SORBS1*
4/50	$1.559e^{-2}$	Body mass index procedure	*ADCY3, COL24A1, RSPO3, SYN2*
20/536	$1.597e^{-2}$	Body mass index	*ADCY3, AGBL4, ASIC2, CDH13, CDYL, CHAF1A, CHRNB4, COL24A1, DLG2, EBF1, EPHB1, GALNT16, LIPC, MIR583HG, PBRM1, PTPRD, SORBS1, SYN2, TNRC6C, ZSWIM6*

Table S4. Functional enrichment analysis of DPpGCs overrepresented in TA based on the DisGeNET annotation. Number of genes in the signal set 155. Number of genes in the background set 10771.

Count	*p*-value	DisGeNET	Genes
5/41	$3.920e^{-4}$	Restless Legs Syndrome	*MFN2, PCDHA3, RNMT, SLC25A37, ZC4H2*
6/63	$4.609e^{-4}$	Neutrophil count (procedure)	*PCDHA1, PCDHA2, PCDHA3, PCDHA4, PIK3R3, THADA*
5/56	$1.674e^{-3}$	Creatinine measurement, serum (procedure)	*DACH1, JPH2, LMCD1-AS1, SIPA1L3, THADA*
9/170	$2.010e^{-3}$	Glomerular Filtration Rate	*CA12, DACH1, JPH2, NEB, PIK3R3, SIMC1, SIPA1L3, SND1, THADA*
6/92	$3.355e^{-3}$	Birth Weight	*CDKAL1, ITPR2, ME1, OBI1-AS1, SLC25A37, SND1*
7/122	$3.550e^{-3}$	Blood basophil count (lab test)	*P4HA2, PCDHA1, PCDHA2, PCDHA3, PCDHA4, THADA, TNIP1*
33/1178	$4.870e^{-3}$	Tumor Progression	*ADAM10, AK2, ATAD3B, CA12, CDCP1, CDH1, CDH17, DACH1, DIAPH3, DLEU1, FUT8, GNAI2, GPR39, KCNH5, LGR5, LINC00536, LRIG2, MAP4K5, MFN2, PIBF1, PIK3R3, PLXDC1, PPFIBP1, REST, RGS17, ROR2, RPS6KA1, SND1, SNX9, TMPRSS4, TRPV1, VAV3, ZC4H2*
9/199	$5.711e^{-3}$	Serum albumin measurement	*ABCB11, ADAM10, CDKAL1, ITPR2, NKAIN3, PCDHA1, PCDHA2, PCDHA3, PCDHA4*
4/50	$6.477e^{-3}$	Convulsions	*ME1, MFN2, REST, TBCD*
11/276	$6.730e^{-3}$	Finding of Mean Corpuscular Hemoglobin	*CDH1, CDKAL1, ITPR2, NEB, PIBF1, PIK3R3, RPS6KA1, SLC25A37, TBC1D4, THADA USP4*
4/54	$8.519e^{-3}$	Arthrogryposis	*NEB, ROR2, TBCD, ZC4H2*
9/222	$1.131e^{-2}$	Vital capacity	*CCNT2-AS1, DIAPH3, DLEU1, JPH2, LMCD1-AS1, PCDHA1, PCDHA2, PCDHA3, PCDHA4*
4/59	$1.162e^{-2}$	Atrial Premature Complexes	*CDH1, LGR5, SND1, TRPV1*
5/88	$1.175e^{-2}$	Substance Dependence	*CDCP1, CSMD3, FAM184A, KLF12, RGS17*
6/122	$1.303e^{-2}$	Uric acid measurement (procedure)	*CDKAL1, DACH1, INMT-MINDY4, LINC01229, MINDY4, SIPA1L3*
4/61	$1.304e^{-2}$	Clinodactyly	*CDH1, PAH, PGAP3, ROR2*
4/62	$1.379e^{-2}$	Prediabetes syndrome	*CDKAL1, DACH1, MFN2, TBC1D4*
22/772	$1.437e^{-2}$	Malignant neoplasm of pancreas	*ACO1, ADAM10 ,CDCP1, CDH1, CDH17, CDKAL1, CLCA1, DACH1, GFRA2, KLF12, MAP4K5, MFN2, P4HA2, PIK3R3, PPFIBP1, REST, ROR2, RPS6KA1, SLC25A37, TNIP1, TRPV1, VAV3*
4/66	$1.706e^{-2}$	Hematocrit procedure	*CCNT2-AS1, DLEU1, HYDIN, TMEM163*
5/97	$1.738e^{-2}$	HER2-positive carcinoma of breast	*ADAM10, CA12, CDCP1, PIK3R3, SFMBT2*
13/401	$1.853e^{-2}$	Secondary malignant neoplasm of lung	*ADAM10, CA12, CAPRIN1, CDCP1, CDH1, CDH17, FUT8, P4HA2, RPS6KA1, SLC25A37, SND1, TMPRSS4, VAV3*
49/2079	$1.947e^{-2}$	Malignant neoplasm of breast	*ABCB11, ADAM10, ATAD3B, CA12, CAPRIN1, CDCP1, CDH1, CDH17, CDKAL1, CLCA1, DACH1, DIAPH3, DLEU1, FUT8, GNAI2, GPR39, GRK4, LGR5, LINC01483, MAPK10, MFN2, MINDY4, P4HA2, PAH, PGAM1P5, PGAP3, PIBF1, PIK3R3, PPP2R5E, REST, RFTN1, RGS17, RNMT, ROR2, RPS6KA1, SLC25A37, SLC48A1, SND1, SNX9, STRBP, TAFA4, TMPRSS4, TNIP1, TRPV1, USP4, VAV3, ZNF131, ZNF516, ZSWIM5*
5/100	$1.959e^{-2}$	Drug habituation	*CDCP1, CSMD3, FAM184A, KLF12, SND1*
5/103	$2.199e^{-2}$	Liver regeneration disorder	*ADAM10, CDH1, LGR5, MAPK10, PAH*
9/251	$2.328e^{-2}$	Eosinophil count procedure	*DLEU1, LINC01229, LINC02391, P4HA2, PIK3R3, SIPA1L3, THADA, TNIP1, VAV3*
20/724	$2.459e^{-2}$	Adenocarcinoma of lung (disorder)	*AK2, ATAD3B, CA12, CDCP1, CDH1, DACH1, DIAPH3, LMCD1-AS1, MFN2, MINDY4, PIK3R3, RGS17, RPS6KA1, SH3RF1, SIPA1L3, SLC4A4, SND1, STRBP, TMPRSS4, USP4*
4/74	$2.498e^{-2}$	Organic Mental Disorders, Substance-Induced	*CDCP1, CSMD3, FAM184A, KLF12*
4/74	$2.498e^{-2}$	Absent reflex	*MFN2, NEB, TBCD, ZC4H2*

Table S5. Functional enrichment analysis of DPpGCs overrepresented in TS based on the GSEA annotation. Number of genes in the signal set 158. Number of genes in the background set 10771.

Count	*p*-value	GSEA	Genes
5/28	$2.285e^{-4}$	protein autoubiquitination	*LRRK2, RNF157, RNF213, UBE2D2, UBE2D3*
3/8	$3.282e^{-4}$	retrograde axonal transport	*AGBL4, DLG2, DST*
5/31	$3.769e^{-4}$	neuron projection cytoplasm	*AGBL4, AP3M1, DLG2, DST, LRRK2*
2/3	$7.986e^{-4}$	regulation of transmission of nerve impulse	*CHRNB4, FGF12*
2/3	$7.986e^{-4}$	cellular response to manganese ion	*BACE1, LRRK2*
4/22	$8.166e^{-4}$	axon cytoplasm	*AGBL4,,AP3M1, DLG2, DST*
8/95	$1.030e^{-3}$	cytoplasmic region	*AGBL4, AP3M1, DLG2, DNAH17, DNAH7, DST, LRRK2, WDR35*
5/39	$1.126e^{-3}$	single fertilization	*ADCY3, AR, SYT6, TRPC6, WDR48*
3/12	$1.230e^{-3}$	regulation of establishment of protein localization to mitochondrion	*LRRK2, NMT1, UBE2D3*
2/4	$1.585e^{-3}$	cellular response to testosterone stimulus	*AR, MSN*
2/4	$1.585e^{-3}$	intrinsic hand muscle atrophy	*FLNC, RYR1*
9/128	$1.966e^{-3}$	microtubule based movement	*ADCY3, AGBL4, AP3M1, CFAP44, DLG2, DNAH17, DNAH7, DST, WDR35*
6/63	$2.014e^{-3}$	sodium ion transmembrane transport	*ASIC2, ATP1A3, FGF12, HECW1, SLC17A7, SLC6A11*
2/5	$2.621e^{-3}$	seminiferous tubule development	*AR, WDR48*
2/5	$2.621e^{-3}$	megaloblastic anemia	*LMBRD1, PHGDH*
2/5	$2.621e^{-3}$	choroid plexus cyst	*PHGDH, ZSWIM6*
3/16	$2.985e^{-3}$	phototransduction	*ABCA4, ASIC2, NMT1*
3/16	$2.985e^{-3}$	anterograde axonal transport	*AGBL4, AP3M1, DLG2*
3/16	$2.985e^{-3}$	upper limb amyotrophy	*CYP7B1, FLNC, RYR1*
3/16	$2.985e^{-3}$	flushing	*ATP1A3, RUNX1, RYR1*
4/31	$3.090e^{-3}$	gait imbalance	*ATXN10, FLNC, LRRK2, SPTLC2*
6/69	$3.213e^{-3}$	neurotransmitter transport	*BACE1, CHRNB4, LRRK2, SLC17A7, SLC6A11, SYN2*
4/32	$3.481e^{-3}$	lysosomal transport	*AP3M1, DENND3, LRRK2, RNF157*
3/17	$3.581e^{-3}$	central nervous system neuron axonogenesis	*ARHGAP35, EPHB1, PLXNA4*
3/17	$3.581e^{-3}$	synaptic vesicle localization	*AP3M1, LRRK2, SYN2*
15/304	$3.826e^{-3}$	organelle assembly	*ARHGAP35, ATXN10, CFAP44, DNAH17, DNAH7, FLNC LRRK2, MSN, PTPRD, RNF213, STX18, TBC1D14, TPX2, WDR35, WWTR1*

Table S6. Functional enrichment analysis of DPpGCs overrepresented in TA based on the GSEA annotation. Number of genes in the signal set 155. Number of genes in the background set 10771.

Count	*p*-value	GSEA	Genes
2/2	$1.369e^{-4}$	regulation of growth rate	*RFTN1, TMPRSS4*
2/4	$8.124e^{-4}$	negative regulation of calcium ion dependent exocytosis	*GNAI2, REST*
2/5	$1.346e^{-3}$	fucose catabolic process	*FUT10, FUT8*
3/17	$1.369e^{-3}$	membrane protein ectodomain proteolysis	*ADAM10, LRIG2, SNX9*
13/317	$1.858e^{-3}$	metal ion transport	*CLCA1, GNAI2, HECW2, ITPR2, JPH2, KCNH5, NKAIN3, SLC25A37, SLC48A1, SLC4A4, THADA, TMEM163, TRPV1*
3/19	$1.919e^{-3}$	death in childhood	*ABCB11, JPH2, NEB*
9/179	$2.034e^{-3}$	infantile onset	*ABCB11, CA12, HYDIN, MFN2, NEB, PGAP3, REST, TBCD, VPS45*
3/20	$2.238e^{-3}$	phosphatidylinositol 3 phosphate binding	*JPH2, SNX24, ZFYVE28*
4/45	$3.690e^{-3}$	integrin mediated signaling pathway	*ADAM10, CDH17, FUT8, VAV3*
4/45	$3.690e^{-3}$	regulation of dendrite development	*CAPRIN1, COBL, CSMD3, HECW2*
2/8	$3.707e^{-3}$	regulation of membrane protein ectodomain proteolysis	*LRIG2, SNX9*
2/8	$3.707e^{-3}$	calcium release channel activity	*ITPR2, TRPV1*
2/8	$3.707e^{-3}$	duplication of the distal phalanx of hand	*PAH, ROR2*
6/99	$3.775e^{-3}$	phosphatidylinositol binding	*ITPR2, JPH2, SNX24, SNX9, TRPV1, ZFYVE28*
6/100	$3.969e^{-3}$	homophilic cell adhesion via plasma membrane adhesion molecules	*CDH1, CDH17, PCDHA1, PCDHA2, PCDHA3, PCDHA4*
7/133	$4.345e^{-3}$	cadherin binding	*CDH1, CDH17, DIAPH3, DOCK9, PPFIBP1, SND1, SNX9*
2/9	$4.738e^{-3}$	neuronal stem cell population maintenance	*FUT10, REST*
2/9	$4.738e^{-3}$	phosphatidylinositol 5 phosphate binding	*JPH2, SNX24*
9/210	$5.851e^{-3}$	regulation of proteolysis	*LRIG2, PSME4, REST, RPS6KA1, SH3RF1, SH3RF3, SIMC1, SNX9, TNIP1*
3/28	$6.006e^{-3}$	adherens junction organization	*ADAM10, CDH1, TBCD*
13/370	$6.808e^{-3}$	vesicle membrane	*ABCB11, ADAM10, ATAD3B, CLCA1, ITPR2, MCTP1, ROR2, SLC48A1, SNX24, SNX9, TMEM163, VPS45, ZFYVE28*
2/11	$7.157e^{-3}$	bile acid transmembrane transporter activity	*ABCB11, SLCO1C1*
2/11	$7.157e^{-3}$	abnormal tricuspid valve morphology	*JPH2, ROR2*

Table S7. CPpGCs for the sedentary and active SkM (TS and TA) and their function in SkM.

Gene	Function
ASB5 ankyrin repeat and SOCS box containing 5	Satellite cell-specific, expressed in both quiescent and activated satellite cells (Seale *et al.*, 2004).
LTBP1 latent transforming growth factor beta binding protein 1	Involved in the sequestration of latent TGF-β in the extracellular matrix (ECM) and the regulation of its activation in the extracellular environment (Todorovic & Rifkin, 2012).
PKCE protein kinase C epsilon	Roles at sarcomeres and mitochondria in cardiomyocytes (Scruggs *et al.*, 2014).
PRDM16 PR/SET domain 16	Controls a brown fat/SkM switch (Seale *et al*., 2008).
SYNC syncoilin, intermediate filament protein	Highly expressed in skeletal and cardiac muscle; protein with structural role in striated muscle (Poon *et al*., 2002).
Y_RNA small non-coding RNA	Myoblasts produce small extracellular vesicles (ELV-MB) that contain Y_RNA (Rome *et al.*, 2019).
...	**Upper row genes are common CPpGCs in TS and TA; Lower row other CPpGCs of interest in alphabetic order**
NRXN1 neurexin 1	Required for efficient neurotransmission; Mutations in the gene implicated in nicotine dependence (Ching *et al.*, 2010).
PPP2R2C protein phosphatase 2 regulatory subunit Bgamma	Implicated in the negative control of cell growth and division; downregulated in Alzheimer's disease brains (Leong *et al*., 2020).
PRKCZ protein kinase C zeta	Involved in proliferation, differentiation and secretion cellular processes; regulatory component of the insulin-like growth factor 1 receptor *IGF1R* (Seto *et al*., 2015).
VSNL1 visinin like 1	Neuronal Ca^{2+} sensor protein, tumor suppressor by inhibiting cell proliferation, adhesion, and invasiveness; promoter of axonal differentiation and plasticity (Brackmann *et al*., 2005).

References

1. Amoasii, L.; Holland W.; Sanchez-Ortiz, E.; Baskin, K.K.; Pearson, M.; Burgess, S.C.; Nelson, B.R.; Bassel-Duby, R.;Olson, E.N. A MED13-dependent skeletal muscle gene program controls systemic glucose homeostasis and hepatic metabolism. *Genes Dev*. **2016**, *30*, 434–446.
2. Bégin, S.; Guénard, F.; Tchernof, A.; Deshaies, Y.; Pérusse, L.; Biron, S.; Lescelleur, O.; Biertho, L.; Marceau, S.; Vohl,M.-C. Impact of NMT1 gene polymorphisms on features of the metabolic syndrome among severely obese patients. *Obes. Res. Open J*. **2015**, *2*, 101–110.
3. Bell, M.B.; Bush, Z.; McGinnis, G.R.; Rowe, G.C. Adult skeletal muscle deletion of Mitofusin 1 and 2 impedes exercise performance and training capacity. *J. Appl. Physiol*. (1985). **2019**, *126*, 341–353.
4. Bharti, S.K.; Khan, I.; Banerjee, T.; Sommers, J.A.;Wu, Y.; Brosh, R.M. Jr. Molecular functions and cellular roles of the ChlR1 (DDX11) helicase defective in the rare cohesinopathy Warsaw breakage syndrome. *Cell Mol. Life Sci*. **2014**, *71*,2625–2639.
5. Brackmann, M.; Schuchmann, S.; Anand, R.; Braunewell, K.H. Neuronal Ca2+ sensor protein VILIP-1 affects cGMP signalling of guanylyl cyclase B by regulating clathrin-dependent receptor recycling in hippocampal neurons. *J. Cell Sci*. **2005**, *118*, 2495–2505.
6. Chen, M.; Zhang, W.; Lu, X.; Hoggatt, A.M.; Gunst, S.J.; Kassab, G.S.; Tune, J.D.; Herring, B.P. Regulation of 130-kDa Smooth Muscle Myosin Light Chain Kinase Expression by an Intronic CArG Element. *J. Biol. Chem.* **2013**, *288*, 34647–3457.
7. Ching, M.S.; Shen, Y.; Tan, W.H.; Jeste, S.S.; Morrow, E.M.; Chen, X.; Mukaddes, N.M.; Yoo, S.Y.; Hanson, E.; Hundley, R.; et al. Children's Hospital Boston Genotype Phenotype Study Group. Deletions of NRXN1 (neurexin-1) predispose to a wide spectrum of developmental disorders. *Am. J. Med. Genet B Neuropsychiatr. Genet.* **2010**, *153B*, 937–947.
8. Choi, W.I.; Yoon, J.H.; Choi, S.H.; Jeon, B.N.; Kim, H.; Hur, M.W. Proto-oncoprotein Zbtb7c and SIRT1 repression: implications in high-fat diet-induced and age-dependent obesity. *Exp. Mol. Med.* **2021**, *53*, 917–932.

9. Cheret, C.; Willem, M.; Fricker, F.R.; Wende, H.; Wulf-Goldenberg, A.; Tahirovic, S.; Nave, K.A.; Saftig, P.; Haass, C.; Garratt, A.N.; Bennett, D.L.; et al. Bace1 and Neuregulin-1 cooperate to control formation and maintenance of muscle spindles. *EMBO J*. **2013**, *32*, 2015–2028.
10. Faralli, H.; Martin, E.; Coré, N.; Liu, Q.C.; Filippi, P.; Dilworth, F.J.; Caubit, X.; Fasano, L. Teashirt-3, a novel regulator of muscle differentiation, associates with BRG1-associated factor 57 (BAF57) to inhibit myogenin gene expression. *J. Biol. Chem*. **2011**, *286*, 23498–23510.
11. Grarup, N.; Moltke, I.; Andersen, M.K.; Dalby, M.; Vitting-Seerup, K.; Kern, T.; Mahendran, Y.; Jørsboe, E.; Larsen, C.V.L.; Dahl-Petersen, I.K.; et al. Loss-of-function variants in ADCY3 increase risk of obesity and type 2 diabetes. *Nat. Genet*. **2018**, *50*, 172–174.
12. Joshi, A.S.; Ragusa, J.V.; Prinz, W.A.; Cohen, S. Multiple C2 domain-containing transmembrane proteins promote lipid droplet biogenesis and growth at specialized endoplasmic reticulum subdomains. *Mol. Biol. Cell.* **2021**, *32*, 1147–1157.
13. Jung, T.W.; Park, J.; Sun, J.L.; Ahn, S.H.; Abd El-Aty, A.M.; Hacimuftuoglu, A.; Kim, H.C.; Shim, J.H.; Shin, S.; Jeong, J.H. Administration of kynurenic acid reduces hyperlipidemia-induced inflammation and insulin resistance in skeletal muscle and adipocytes. *Mol. Cell Endocrinol*. **2020**, *518*, 110928.
14. Kamizaki, K.; Endo, M.; Minami, Y.; Kobayashi, Y. Role of noncanonical Wnt ligands and Ror-family receptor tyrosine kinases in the development, regeneration, and diseases of the musculoskeletal system. Dev. Dyn. 2021, 250, 27-38.
15. Kim, J.; Kim, J.; Min, H.; Oh, S.; Kim, Y.; Lee, A.H.; Park, T. Joint identification of genetic variants for physical activity in Korean population. *Int. J. Mol. Sci*. **2014**, *15*, 12407–12421.
16. Kotani, Y.; Morito, D.; Yamazaki, S.; Ogino, K.; Kawakami, K.; Takashima, S.; Hirata, H.; Nagata, K. Neuromuscular regulation in zebrafish by a large AAA+ ATPase/ubiquitin ligase, mysterin/RNF213. *Sci. Rep*. **2015**, *5*, 16161.
17. Leong, W.; Xu, W.; Wang, B.; Gao, S.; Zhai, X.; Wang, C.; Gilson, E.; Ye, J.; Lu, Y. PP2A subunit PPP2R2C is downregulated in the brains of Alzheimer's transgenic mice. *Aging (Albany NY).* **2020**, *12*, 6880–-6890.
18. Li, C.; Mo, D.; Li, M.; Zheng, Y.; Li, Q.; Ou, S.; Zhang, Z. Age-related but not longevity-related genes are found by weighted gene co-expression network analysis in the peripheral blood cells of humans. *Genes Genet. Syst*. **2019**, *93*, 221–228.
19. Mizuno, S.; Yoda, M.; Shimoda, M.; Tohmonda, T.; Okada, Y.; Toyama, Y.; Takeda, S.; Nakamura, M.; Matsumoto, M.; Horiuchi, K. A Disintegrin and Metalloprotease 10 (ADAM10) Is Indispensable for Maintenance of the Muscle Satellite Cell *Pool. J. Biol. Chem*. **2015**, *290*, 28456–28464.
20. Ndiaye, F.K.; Huyvaert, M.; Ortalli, A.; Canouil, M.; Lecoeur, C.; Verbanck, M.; Lobbens, S.; Khamis, A.; Marselli, L.; Marchetti, P.; et al. The expression of genes in top obesity-associated loci is enriched in insula and substantia nigra brain regions involved in addiction and reward. *Int. J. Obes (Lond)*. **2020**, *44*, 539–543.
21. Palmer, C.J.; Bruckner, R.J.; Paulo, J.A.; Kazak, L.; Long, J.Z.; Mina, A.I.; Deng, Z.; LeClair, K.B.; Hall, J.A.; Hong, S.; et al. Cdkal1, a type 2 diabetes susceptibility gene, regulates mitochondrial function in adipose tissue. *Mol. Metab*. **2017**, *6*, 1212–1225.
22. Pan, H.; Xu, X.; Wu, D.; Qiu, Q.; Zhou, S.; He, X.; Zhou, Y.; Qu, P.; Hou, J.; He, J.; et al. Novel somatic mutations identified by whole-exome sequencing in muscle-invasive transitional cell carcinoma of the bladder. *Oncol. Lett.* **2016**, *11*, 1486-1492.
23. Peres de Oliveira, A.; Kazuo Issayama, L.; Betim Pavan, I.C.; Riback Silva, F.; Diniz Melo-Hanchuk, T.; Moreira Simabuco, F.; Kobarg, J. Checking NEKs: Overcoming a Bottleneck in Human Diseases. *Molecules.* **2020**, *25*, 1778.
24. Polge, C.; Attaix, D.; Taillandier, D. Role of E2-Ub-conjugating enzymes during skeletal muscle atrophy. *Front. Physiol*. **2015**, *6*, 59.
25. Poon, E.; Howman, E.V.; Newey, S.E.; Davies, K.E. Association of syncoilin and desmin: linking intermediate filament proteins to the dystrophin-associated protein complex. *J. Biol. Chem.* **2002**, *277*, 3433–3439. 1226.
26. Radom-Aizik, S.; Zaldivar, F. Jr.; Leu, S.Y.; Cooper, D.M. Brief bout of exercise alters gene expression in peripheral blood mononuclear cells of early- and late-pubertal males. *Pediatr. Res*. **2009**, *65*, 447–452.
27. Rogowski, K.; van Dijk, J.; Magiera, M.M.; Bosc, C.; Deloulme, J.C.; Bosson, A.; Peris, L.; Gold, N.D.; Lacroix, B.; Bosch Grau, M.; et al. A Family of Protein-Deglutamylating Enzymes Associated with Neurodegeneration. *Cell*. **2010**, *143*, 564–578.
28. Rome, S.; Forterre, A.; Mizgier, M.L.; Bouzakri, K. Skeletal Muscle-Released Extracellular Vesicles: State of the Art. *Front. Physiol*. **2019**, *10*, 929.
29. Rusu, V.; Hoch, E.; Mercader, J.M.; Tenen, D.E.; Gymrek, M.; Hartigan, C.R.; DeRan, M.; von Grotthuss, M.; Fontanillas, P.; Spooner, A.; et al. Type 2 Diabetes Variants Disrupt Function of SLC16A11 through Two Distinct Mechanisms. *Cell*. **2017**, *170*, 199–212.e20.
30. Sarkar, P.; Thirumurugan, K. New insights into TNFα/PTP1B and PPARγ pathway through RNF213- a link between inflammation, obesity, insulin resistance, and Moyamoya disease. *Gene*. **2021**, *771*, 145340.
31. Scruggs, S.B.; Wang, D.; Ping, P. PRKCE gene encoding protein kinase C-epsilon-Dual roles at sarcomeres and mitochondria in cardiomyocytes. *Gene*. **2016**, *590*, 90–96.
32. Seale, P.; Bjork, B.; Yang, W.; Kajimura, S.; Chin, S.; Kuang, S.; Scimè, A.; Devarakonda, S.; Conroe, H.M.; Erdjument-Bromage, H.; et al. PRDM16 controls a brown fat/skeletal muscle switch. *Nature*. **2008**, *454*, 961–967.
33. Selman, C.; Tullet, J.M.; Wieser, D.; Irvine, E.; Lingard, S.J.; Choudhury, A.I.; Claret, M.; Al-Qassab, H.; Carmignac, D.; Ramadani, F.; et al. Ribosomal protein S6 kinase 1 signaling regulates mammalian life span. *Science*. **2009**, *326*, 140–144.
34. Setiawan, I.; Sanjaya, A.; Lesmana, R.; Yen, P.M.; Goenawan, H. Hippo pathway effectors YAP and TAZ and their association with skeletal muscle ageing. *J. Physiol. Biochem.* **2021**, *77*, 63–73.

35. Seto, K.K.; Andrulis, I.L. Atypical protein kinase C zeta: potential player in cell survival and cell migration of ovarian cancer. *PLoS One*. **2015**, *10*, e0123528.
36. Shamilov, R.; Aneskievich, B.J. TNIP1 in Autoimmune Diseases: Regulation of Toll-like Receptor Signaling. *J. Immunol. Res*. **2018**, *2018*, 3491269.
37. Söhle, J.; Machuy, N.; Smailbegovic, E.; Holtzmann, U.; Grönniger, E.; Wenck, H.; Stäb, F.; Winnefeld, M. Identification of new genes involved in human adipogenesis and fat storage. *PLoS One*. **2012**, *7*, e31193.
38. Sun, C.; De Mello, V.; Mohamed, A.; Ortuste Quiroga, H.P.; Garcia-Munoz, A.; Al Bloshi, A.; Tremblay, A.M.; von Kriegsheim, A.; Collie-Duguid, E.; Vargesson, N.; et al. Common and Distinctive Functions of the Hippo Effectors Taz and Yap in Skeletal Muscle Stem Cell Function. *Stem Cells.* **2017**, *35*, 1958–1972.
39. Thiel, G. Synapsin I, synapsin II, and synaptophysin: marker proteins of synaptic vesicles. *Brain Pathol.* **1993**, *3*, 87–95.
40. Todorovic, V.; Rifkin, D.B. LTBPs, more than just an escort service. *J. Cell Biochem.* **2012**, *113*, 410–418.
41. Uezumi, A.; Nakatani, M.; Ikemoto-Uezumi, M.; Yamamoto, N.; Morita, M.; Yamaguchi, A.; Yamada, H.; Kasai, T.; Masuda, S.; Narita, A.; et al. Cell-Surface Protein Profiling Identifies Distinctive Markers of Progenitor Cells in Human Skeletal Muscle. *Stem. Cell Reports*. **2016**, *7*, 263–278.
42. Weng, X.; Lin, D.; Huang, J.T.J.; Stimson, R.H.; Wasserman, D.H.; Kang, L. Collagen 24 α1 Is Increased in Insulin-Resistant Skeletal Muscle and Adipose Tissue. *Int. J. Mol. Sci*. 2020, *21*, 5738.
43. Wiel, C.; Lallet-Daher, H.; Gitenay, D.; Gras, B.; Le Calvé, B.; Augert, A.; Ferrand, M.; Prevarskaya, N.; Simonnet, H.;Vindrieux, D.; et al. Endoplasmic reticulum calcium release through ITPR2 channels leads to mitochondrial calcium accumulation and senescence. *Nat. Commun*. **2014**, *5*, 3792.
44. Witt, C.C.; Burkart, C.; Labeit, D.; McNabb, M.; Wu, Y.; Granzier, H.; Labeit, S. Nebulin regulates thin filament length, contractility, and Z-disk structure in vivo. *EMBO J*. 2006, *25*, 3843–3855.
45. Zhao, Y.; Huang, G.; Chen, Z.; Fan, X.; Huang, T.; Liu, J.; Zhang, Q.; Shen, J.; Li, Z.; Shi, Y. Four Loci Are Associated with Cardiorespiratory Fitness and Endurance Performance in Young Chinese Females. *Sci. Rep*. **2020**, *10*, 10117.
46. Ziegler, D.V.; Vindrieux, D.; Goehrig, D.; Jaber, S.; Collin, G.; Griveau, A.; Wiel, C.; Bendridi, N.; Djebali, S.;Farfariello, V.; et al. Calcium channel ITPR2 and mitochondria-ER contacts promote cellular senescence and aging. *Nat. Commun*. **2021**, *12*, 720.
47. Zykovich, A.; Hubbard, A.; Flynn, J.M.; Tarnopolsky, M.; Fraga, M.F.; Kerksick, C.; Ogborn, D.; MacNeil, L.; Mooney, S.D.; Melov, S. Genome-wide DNA methylation changes with age in disease-free human skeletal muscle. *Aging Cell*. **2014**, *13*, 360–366.

Supplementary Figures

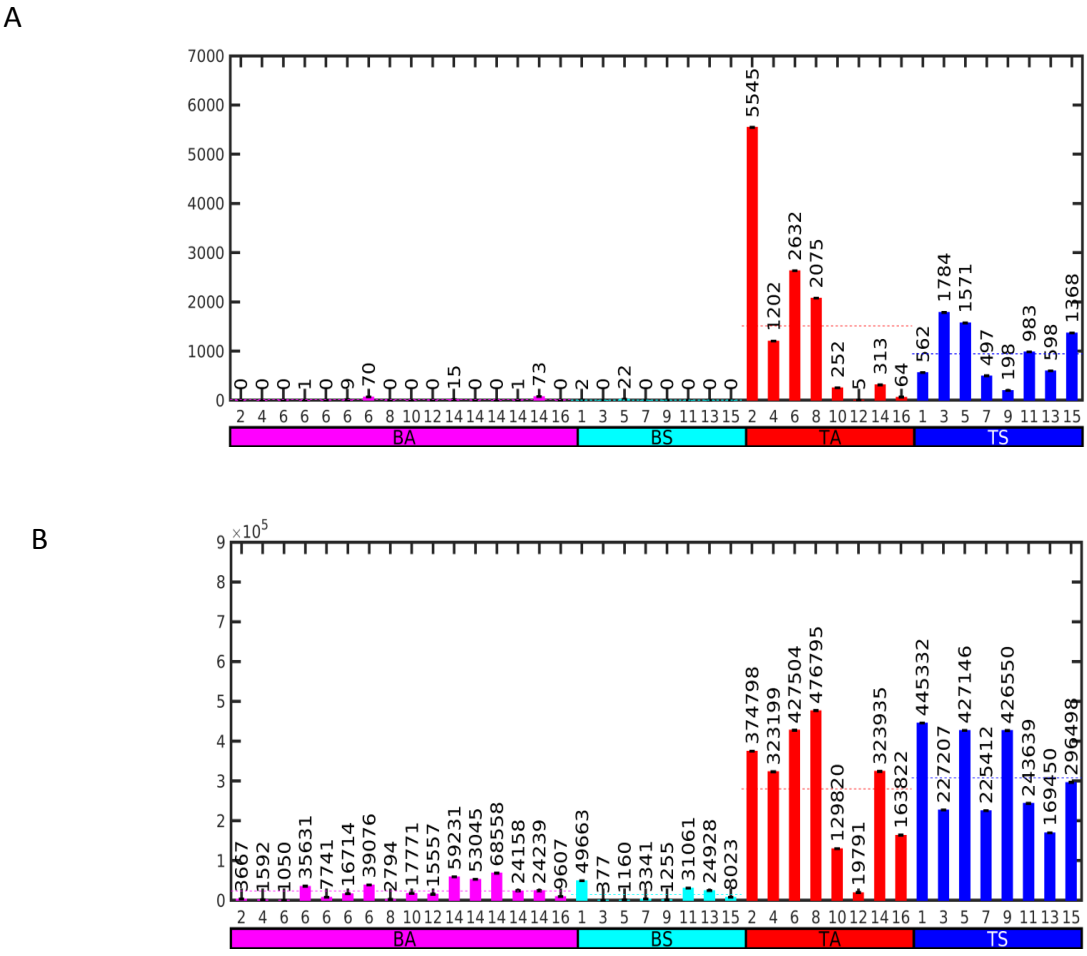

Figure S1. Mitochondrial eccDNA analysis. (A) Number of split reads per sample in mitochondrial eccDNA. (B) Number of split reads per sample in non-mitochondrial eccDNA. The horizontal dotted lines mark the positions of the mean values of each of the four groups (BA, BS, TA, TS).

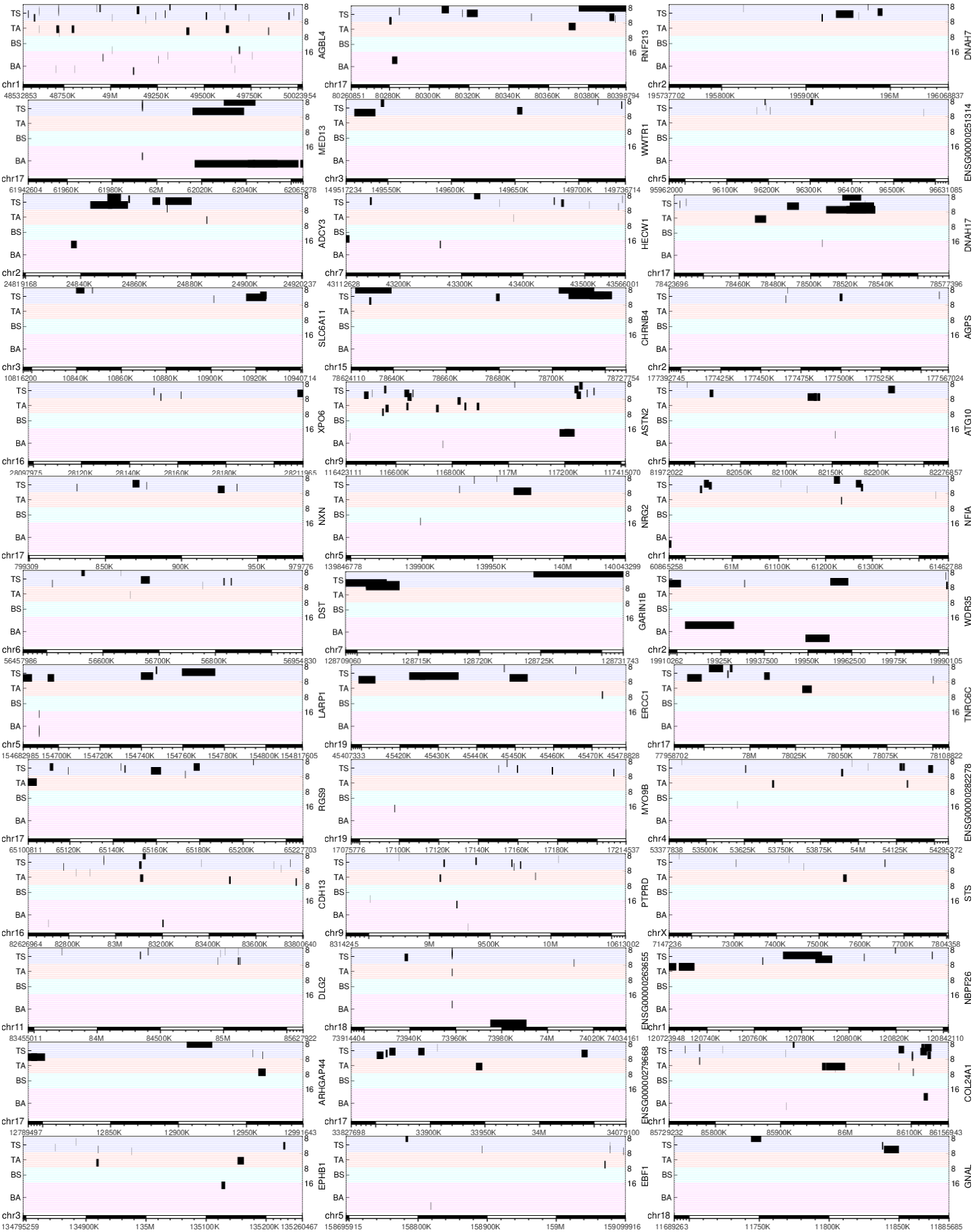
TS
TA
BS
BA
AGBL4
chr1
RNF213
chr17
DNAH7
chr2
MED13
chr17
WWTR1
chr3
ENSG00000251314
chr5
ADCY3
chr2
HECW1
chr7
DNAH17
chr17
SLC6A11
chr3
CHRNB4
chr15
AGPS
chr2
XPO6
chr16
ASTN2
chr9
ATG10
chr5
NXN
chr17
NRG2
chr5
NFIA
chr1
DST
chr6
GARIN1B
chr7
WDR35
chr2
LARP1
chr5
ERCC1
chr19
TNRC6C
chr17
RGS9
chr17
MYO9B
chr19
ENSG00000282278
chr4
CDH13
chr16
PTPRD
chr9
STS
chrX
DLG2
chr11
ENSG00000263655
chr18
NBPF26
chr1
ARHGAP44
chr17
ENSG00000279668
chr17
COL24A1
chr1
EPHB1
chr3
EBF1
chr5
GNAL
chr18

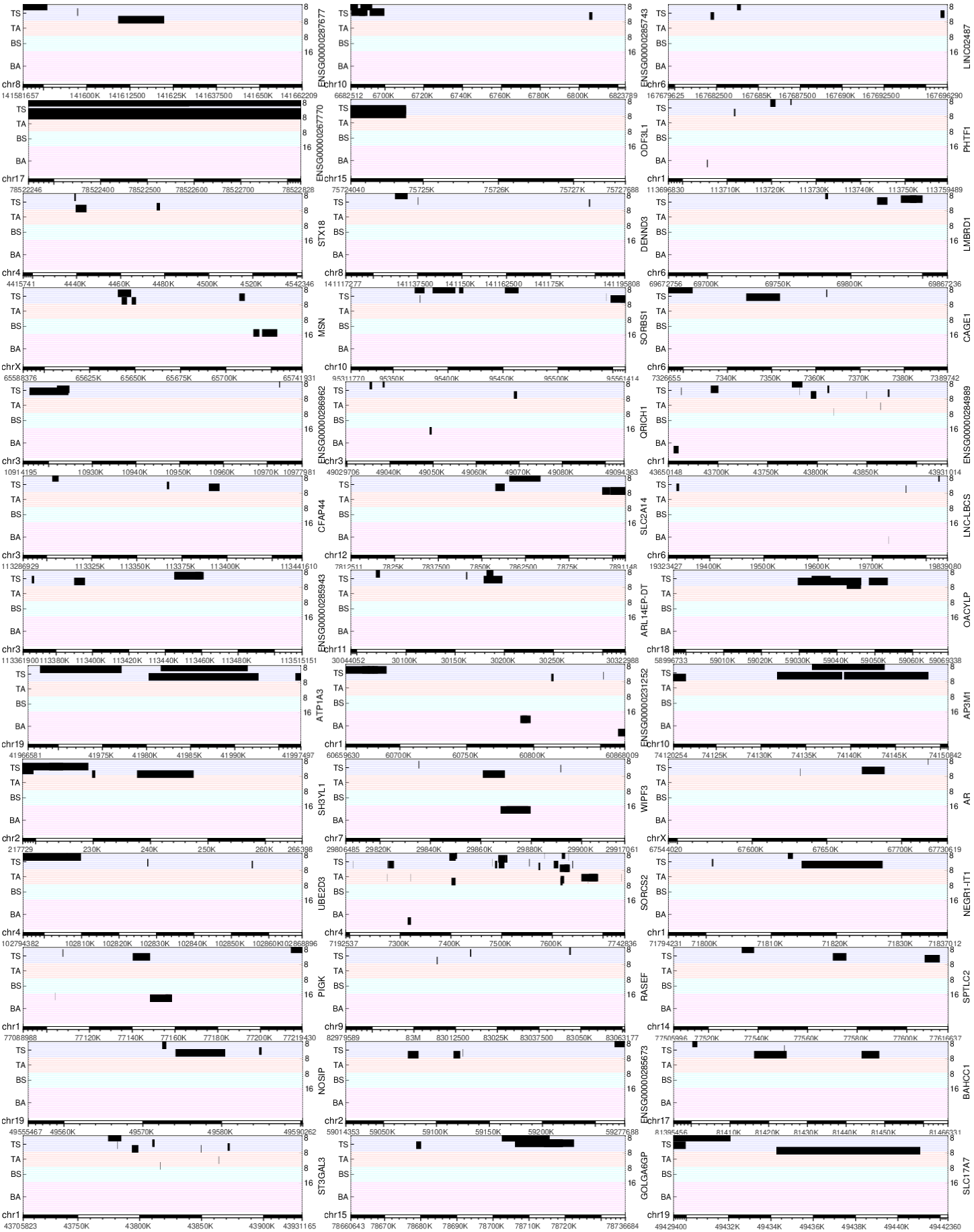
TS
TA
BS
BA
chr8
141581657 141600K 141612500 141625K 141637500 141650K 141662209
ENSG00000287677
chr10
6682512 6700K 6720K 6740K 6760K 6780K 6800K 6823789
ENSG00000285743
chr6
167679625 167682500 167685K 167687500 167690K 167692500 167696290
LINC02487
chr17
78522246 78522400 78522500 78522600 78522700 78522828
ENSG00000267770
chr15
75724040 75725K 75726K 75727K 75727688
ODF3L1
chr1
113696830 113710K 113720K 113730K 113740K 113750K 113759489
PHTF1
chr4
4415741 4440K 4460K 4480K 4500K 4520K 4542346
STX18
chr8
141117277 141137500 141150K 141162500 141175K 141195808
DENND3
chr6
69672756 69700K 69750K 69800K 69867236
LMBRD1
chrX
65588376 65625K 65650K 65675K 65700K 65741931
MSN
chr10
95311770 95350K 95400K 95450K 95500K 95561414
SORBS1
chr6
7326655 7340K 7350K 7360K 7370K 7380K 7389742
CAGE1
chr3
10914195 10930K 10940K 10950K 10960K 10970K 10977981
ENSG00000286962
chr3
49029706 49040K 49050K 49060K 49070K 49080K 49094363
QRICH1
chr1
43650148 43700K 43750K 43800K 43850K 43931014
ENSG00000284989
chr3
113286929 113325K 113350K 113375K 113400K 113441610
CFAP44
chr12
7812511 7825K 7837500 7850K 7862500 7875K 7891148
SLC2A14
chr6
19323427 19400K 19500K 19600K 19700K 19839080
LNC-LBCS
chr3
113361900 113380K 113400K 113420K 113440K 113460K 113480K 113515151
ENSG00000285943
chr11
30044052 30100K 30150K 30200K 30250K 30322988
ARL14EP-DT
chr18
58996733 59010K 59020K 59030K 59040K 59050K 59060K 59069338
OACYLP
chr19
41966581 41975K 41980K 41985K 41990K 41997497
ATP1A3
chr1
60659630 60700K 60750K 60800K 60868009
ENSG00000231252
chr10
74120254 74125K 74130K 74135K 74140K 74145K 74150842
AP3M1
chr2
217729 230K 240K 250K 260K 266398
SH3YL1
chr7
29806485 29820K 29840K 29860K 29880K 29900K 29917061
WIPF3
chrX
67544020 67600K 67650K 67700K 67730619
AR
chr4
102794382 102810K 102820K 102830K 102840K 102850K 102860K 102868896
UBE2D3
chr4
7192537 7300K 7400K 7500K 7600K 7742836
SORCS2
chr1
71794231 71800K 71810K 71820K 71830K 71837012
NEGR1-IT1
chr1
77088988 77120K 77140K 77160K 77180K 77200K 77219430
PIGK
chr9
82979589 83M 83012500 83025K 83037500 83050K 83063177
RASEF
chr14
77506996 77520K 77540K 77560K 77580K 77600K 77616637
SPTLC2
chr19
49555467 49560K 49570K 49580K 49590262
NOSIP
chr2
59014353 59050K 59100K 59150K 59200K 59277688
ENSG00000285673
chr17
81395456 81410K 81420K 81430K 81440K 81450K 81466331
BAHCC1
chr1
43705823 43750K 43800K 43850K 43900K 43931165
ST3GAL3
chr15
78660643 78670K 78680K 78690K 78700K 78710K 78720K 78736684
GOLGA6GP
chr19
49429400 49432K 49434K 49436K 49438K 49440K 49442360
SLC17A7

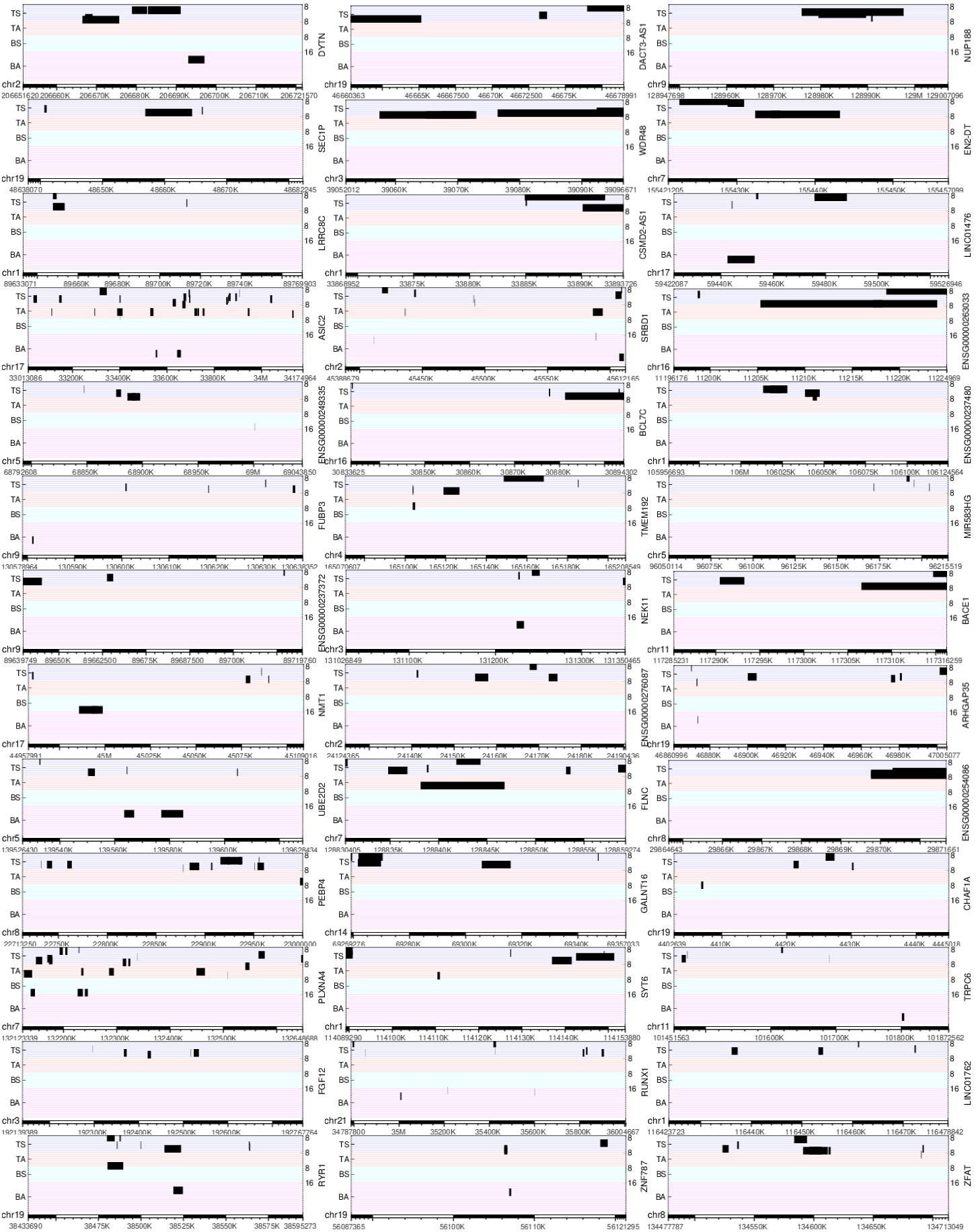
TS
TA
BS
BA
DYTN
NUP188
DACT3-AS1
SEC1P
WDR48
EN2-DT
LRRC8C
CSMD2-AS1
LINC01476
ASIC2
SRBD1
ENSG00000263033
ENSG00000249335
BCL7C
ENSG00000237480
FUBP3
TMEM192
MIR583HG
ENSG00000237372
NEK11
BACE1
NMT1
ENSG00000276087
ARHGAP35
UBE2D2
FLNC
ENSG00000254086
PEBP4
GALNT16
CHAF1A
PLXNA4
SYT6
TRPC6
FGF12
RUNX1
LINC01762
RYR1
ZNF787
ZFAT

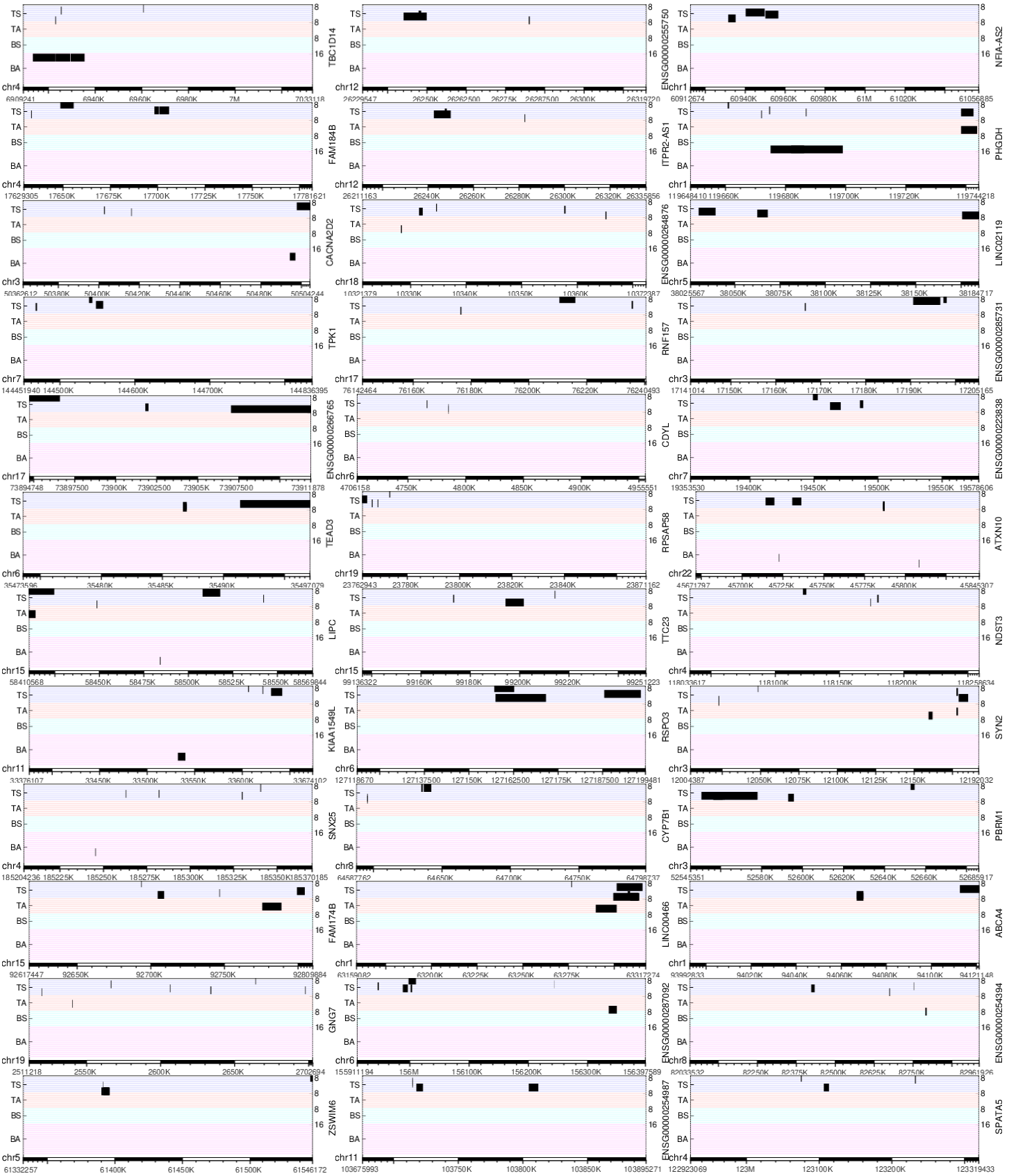
TS
TA
BS
BA
TBC1D14
NFIA-AS2
FAM184B
ITPR2-AS1
PHGDH
CACNA2D2
ENSG00000264876
LINC02119
TPK1
RNF157
ENSG00000285731
ENSG00000266765
CDYL
ENSG00000223838
TEAD3
RPSAP58
ATXN10
LIPC
TTC23
NDST3
KIAA1549L
RSPO3
SYN2
SNX25
CYP7B1
PBRM1
FAM174B
LINC00466
ABCA4
GNG7
ENSG00000287092
ENSG00000254394
ZSWIM6
ENSG00000254987
SPATA5

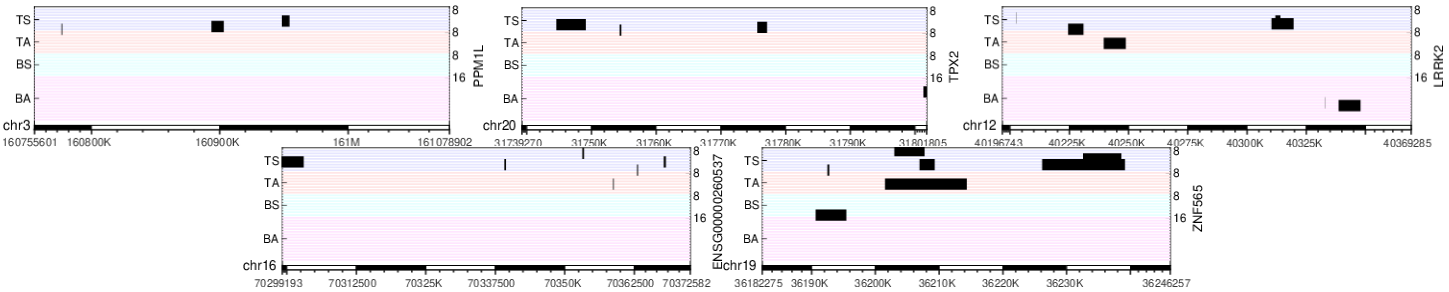

Figure S2. Track plots of the *loci* of the 158 top-ranked up-DPpGCs in TS in relation to TA. The statistically most significant up-DPpGC is *AGBL4* with *p*-value 0.0010762.

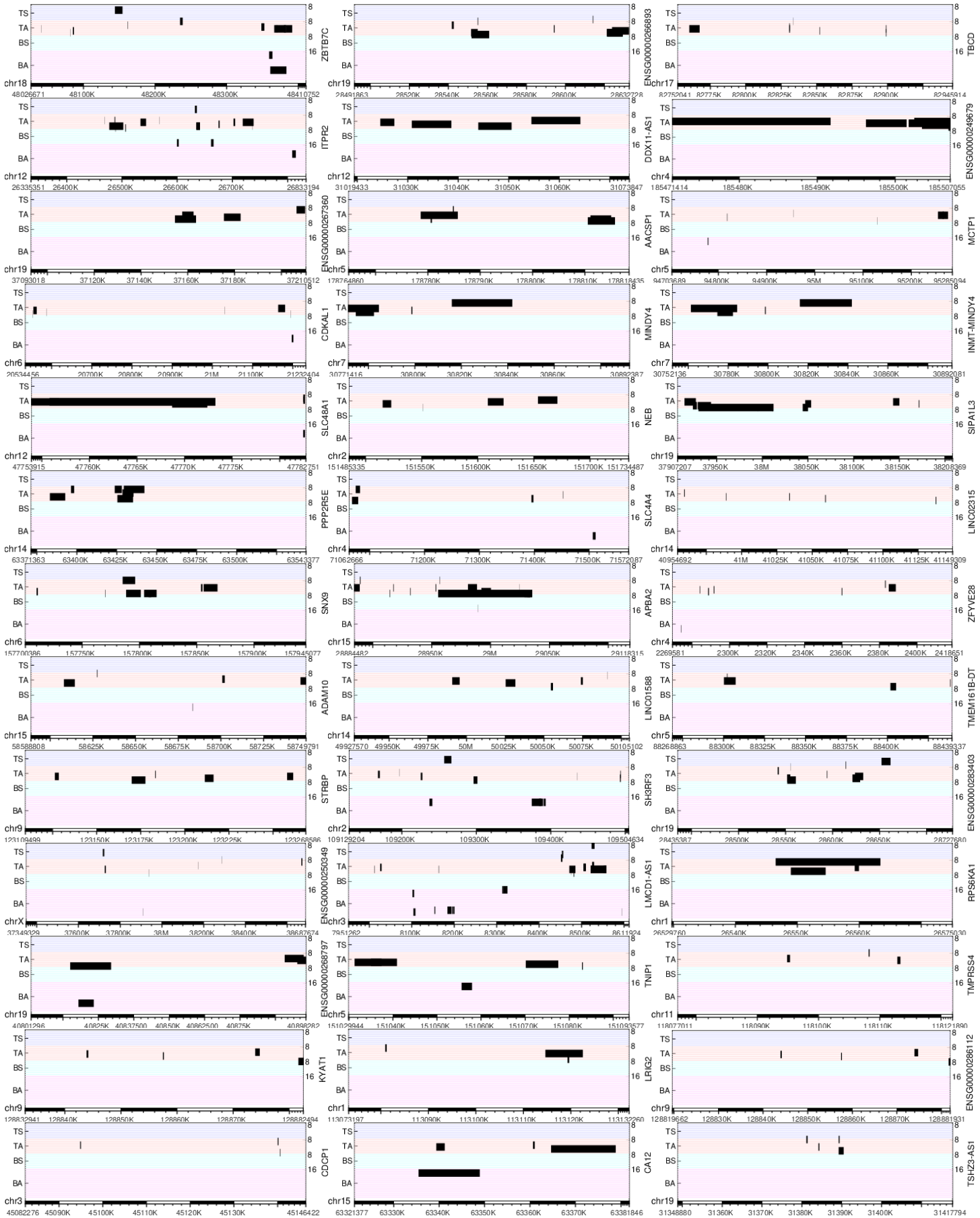
TS
TA
BS
BA
ZBTB7C
chr18
48026671 48100K 48200K 48300K 48410752
ITPR2
chr12
26335351 26400K 26500K 26600K 26700K 26833194
ENSG00000267360
chr19
37093018 37120K 37140K 37160K 37180K 37210512
CDKAL1
chr6
20534456 20700K 20800K 20900K 21M 21100K 21232404
SLC48A1
chr12
47753915 47760K 47765K 47770K 47775K 47782751
PPP2R5E
chr14
63371363 63400K 63425K 63450K 63475K 63500K 63543377
SNX9
chr6
157700386 157750K 157800K 157850K 157900K 157945077
ADAM10
chr15
58588808 58625K 58650K 58675K 58700K 58725K 58749791
STRBP
chr9
123109499 123150K 123175K 123200K 123225K 123268586
ENSG00000250349
chrX
37349329 37600K 37800K 38M 38200K 38400K 38687674
ENSG00000268797
chr19
40801296 40825K 40837500 40850K 40862500 40875K 40898832
KYAT1
chr9
128832941 128840K 128850K 128860K 128870K 128882494
CDCP1
chr3
45082276 45090K 45100K 45110K 45120K 45130K 45146422
ZBTB7C
chr19
28491863 28520K 28540K 28560K 28580K 28600K 28637228
ITPR2
chr12
31019433 31030K 31040K 31050K 31060K 31073847
ENSG00000267360
chr5
178764860 178780K 178790K 178800K 178810K 178818435
CDKAL1
chr7
30771416 30800K 30820K 30840K 30860K 30892387
SLC48A1
chr2
151485335 151550K 151600K 151650K 151700K 151734487
PPP2R5E
chr4
71062666 71200K 71300K 71400K 71500K 71572087
SNX9
chr15
28884482 28950K 29M 29050K 29118315
ADAM10
chr14
49927570 49950K 49975K 50M 50025K 50050K 50075K 50105102
STRBP
chr2
109029204 109200K 109300K 109400K 109504634
ENSG00000250349
chr3
7951262 8100K 8200K 8300K 8400K 8500K 8611924
ENSG00000268797
chr5
151029944 151040K 151050K 151060K 151070K 151080K 151093577
KYAT1
chr1
113073197 113090K 113100K 113110K 113120K 113132260
CDCP1
chr15
63321377 63330K 63340K 63350K 63360K 63370K 63381846
ENSG00000266893
chr17
82752041 82775K 82800K 82825K 82850K 82875K 82900K 82945914
DDX11-AS1
chr4
185471414 185480K 185490K 185500K 185507055
AACSP1
chr5
94709689 94800K 94900K 95M 95100K 95200K 95285094
MINDY4
chr7
30752136 30780K 30800K 30820K 30840K 30860K 30892081
NEB
chr19
37907207 37950K 38M 38050K 38100K 38150K 38208369
SLC4A4
chr14
40954692 41M 41025K 41050K 41075K 41100K 41125K 41149309
APBA2
chr4
2269581 2300K 2320K 2340K 2360K 2380K 2400K 2418651
LINC01588
chr5
88268863 88300K 88325K 88350K 88375K 88400K 88439337
SH3RF3
chr19
28435387 28500K 28550K 28600K 28650K 28727680
LMCD1-AS1
chr1
26529760 26540K 26550K 26560K 26575030
TNIP1
chr11
118077011 118090K 118100K 118110K 118121890
LRIG2
chr9
128819662 128830K 128840K 128850K 128860K 128870K 128881931
CA12
chr19
31348880 31360K 31370K 31380K 31390K 31400K 31417794
TBCD
ENSG00000249679
MCTP1
INMT-MINDY4
SIPA1L3
LINC02315
ZFYVE28
TMEM161B-DT
ENSG00000283403
RPS6KA1
TMPRSS4
ENSG00000286112
TSHZ3-AS1

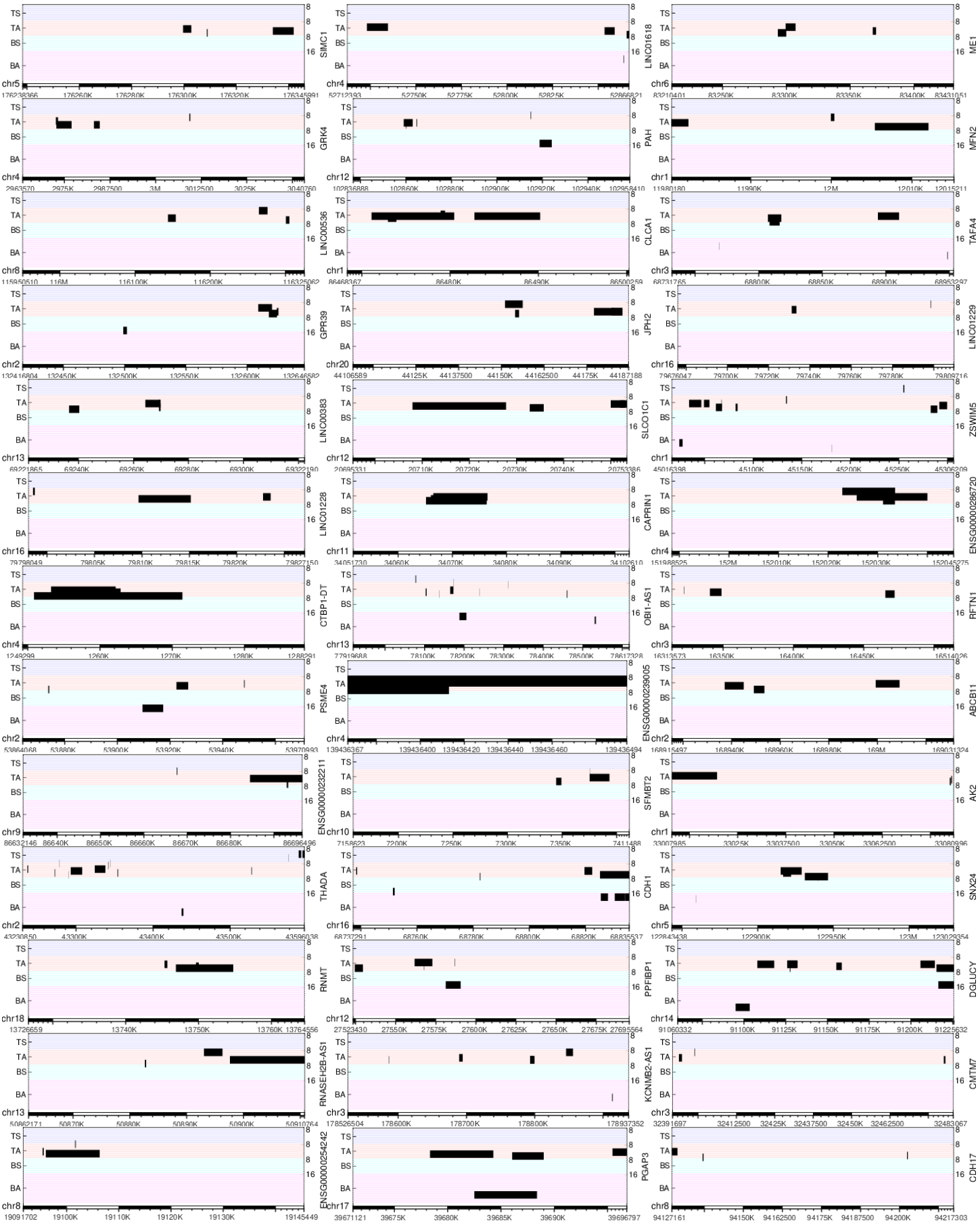
TS
TA
BS
BA
SIMC1
LINC01618
ME1
GRK4
PAH
MFN2
LINC00536
CLCA1
TAFA4
GPR39
JPH2
LINC01229
LINC00383
SLCO1C1
ZSWIM5
LINC01228
CAPRIN1
ENSG00000286720
CTBP1-DT
OBI1-AS1
RFTN1
PSME4
ENSG00000239005
ABCB11
ENSG00000232211
SFMBT2
AK2
THADA
CDH1
SNX24
RNMT
PPFIBP1
DGLUCY
RNASEH2B-AS1
KCNMB2-AS1
CMTM7
ENSG00000254242
PGAP3
CDH17

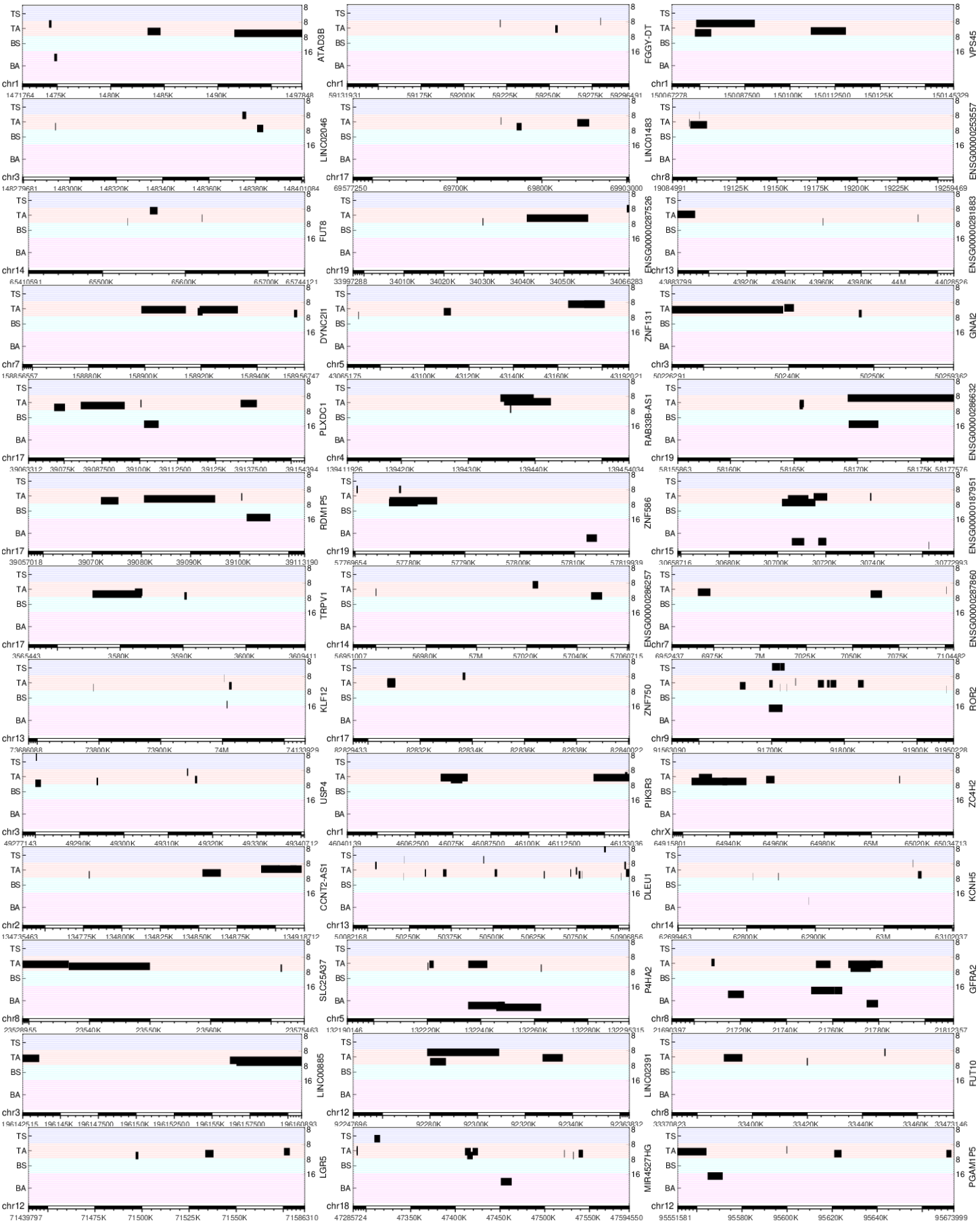
TS
TA
BS
BA
ATAD3B
FGGY-DT
VPS45
LINC02046
LINC01483
ENSG00000253557
FUT8
ENSG00000287526
ENSG00000281883
DYNC2I1
ZNF131
GNAI2
PLXDC1
RAB33B-AS1
ENSG00000286632
RDM1P5
ZNF586
ENSG00000187951
TRPV1
ENSG00000286257
ENSG00000287860
KLF12
ZNF750
ROR2
USP4
PIK3R3
ZC4H2
CCNT2-AS1
DLEU1
KCNH5
SLC25A37
P4HA2
GFRA2
LINC00885
LINC02391
FUT10
LGR5
MIR4527HG
PGAM1P5

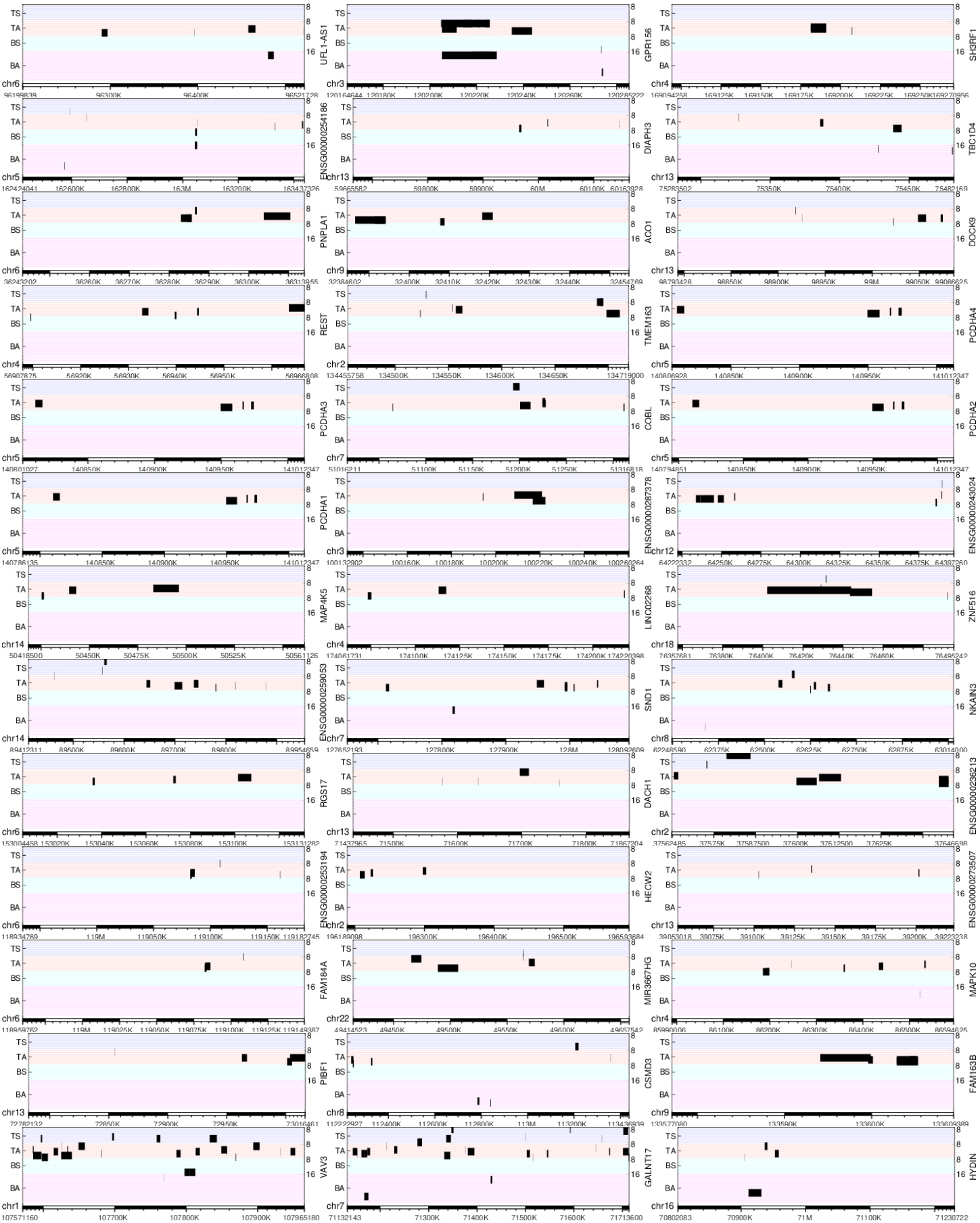

Figure S3. Track plots of the *loci* of the 156 top-ranked up-DPpGCs in TA in relation to TS. The statistically most significant differentially up-DPpGC in TA is *ZBTB7C* with *p*-value 0.0023656.

A

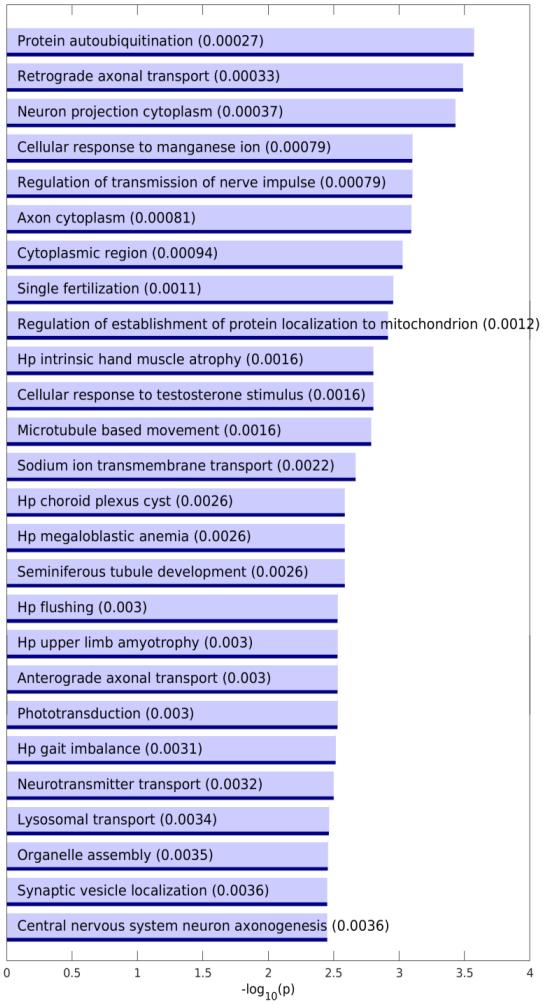

B

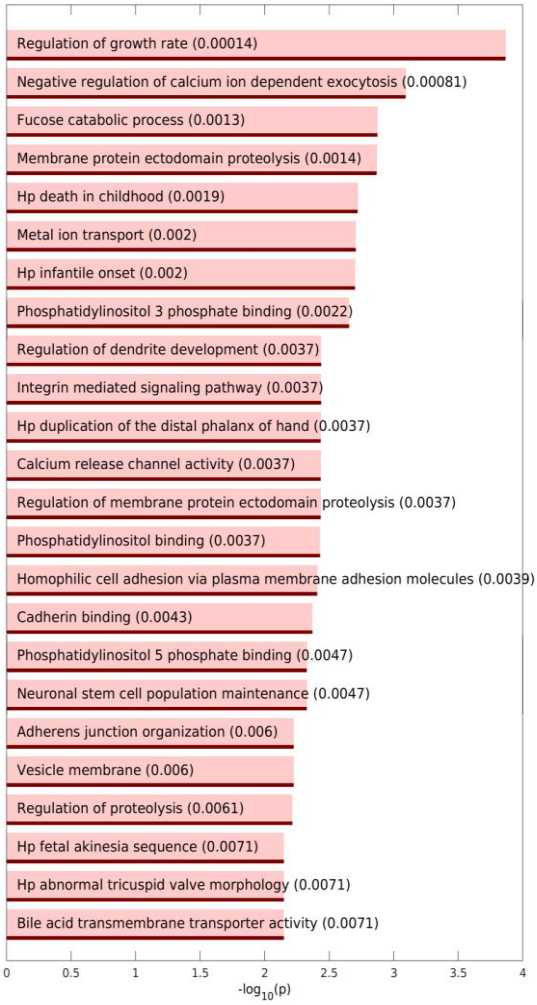

Figure S4. Bar plots of the –log$_{10}$(*p*-value) of the significantly enriched GSEA terms of up-DPpGCs. (A) TS. .(B) TA. Longer bars correspond to higher statistical significance of the enrichment (the *p*-values are given in parentheses).

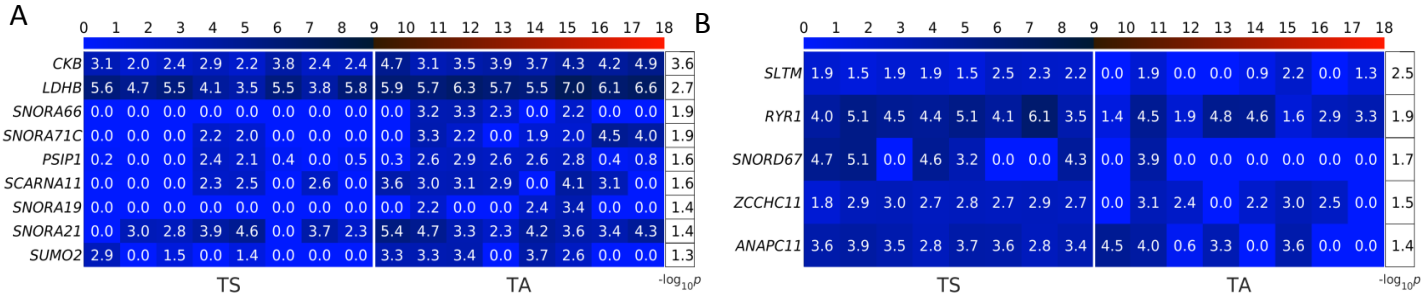

Figure S5. Transcriptomics analysis. Heatmaps of the transcriptomics level of DEGs up-regulated in (A) TA and (B) TS. The color bar codifies the Fragments per Kilobase of Exon per Million Mapped Fragments (FPKMs) in a $\log_{10}$ scale. Higher count corresponds to a redder color.

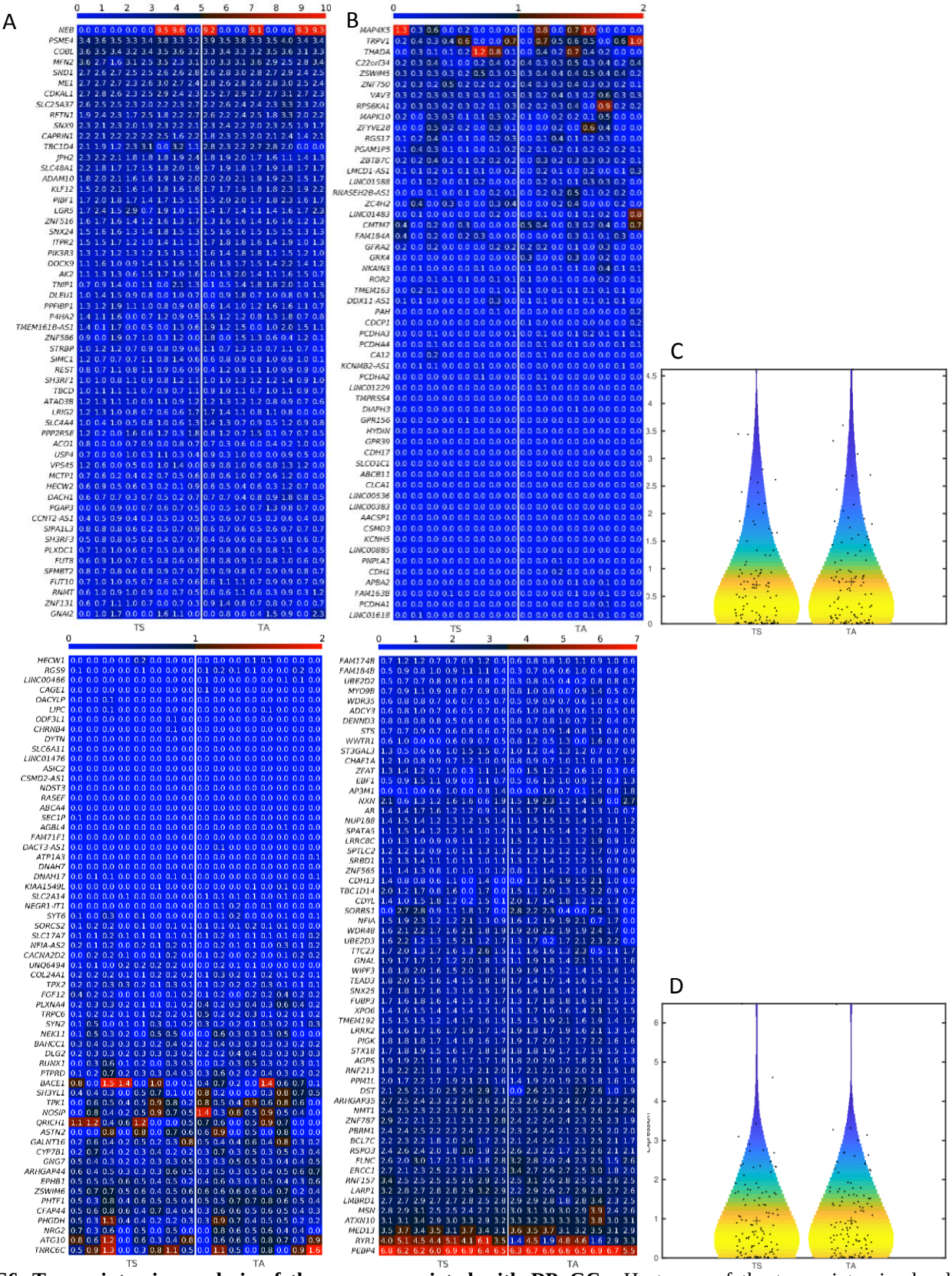

Figure S6. Transcriptomics analysis of the genes associated with DPpGCs. Heatmaps of the transcriptomics level of genes associated with DPpGCs in TS (A) and in TA (B). The color bar codifies the FPKMs in a $\log_{10}$ scale. Higher FPKMs correspond to a redder color. Violins plots associated to the expression distribution of the genes in TS (C) and in TA (D). The black crosses indicate the medians of the distributions. The black points represent the spread of the expression of the genes used to build the distributions.

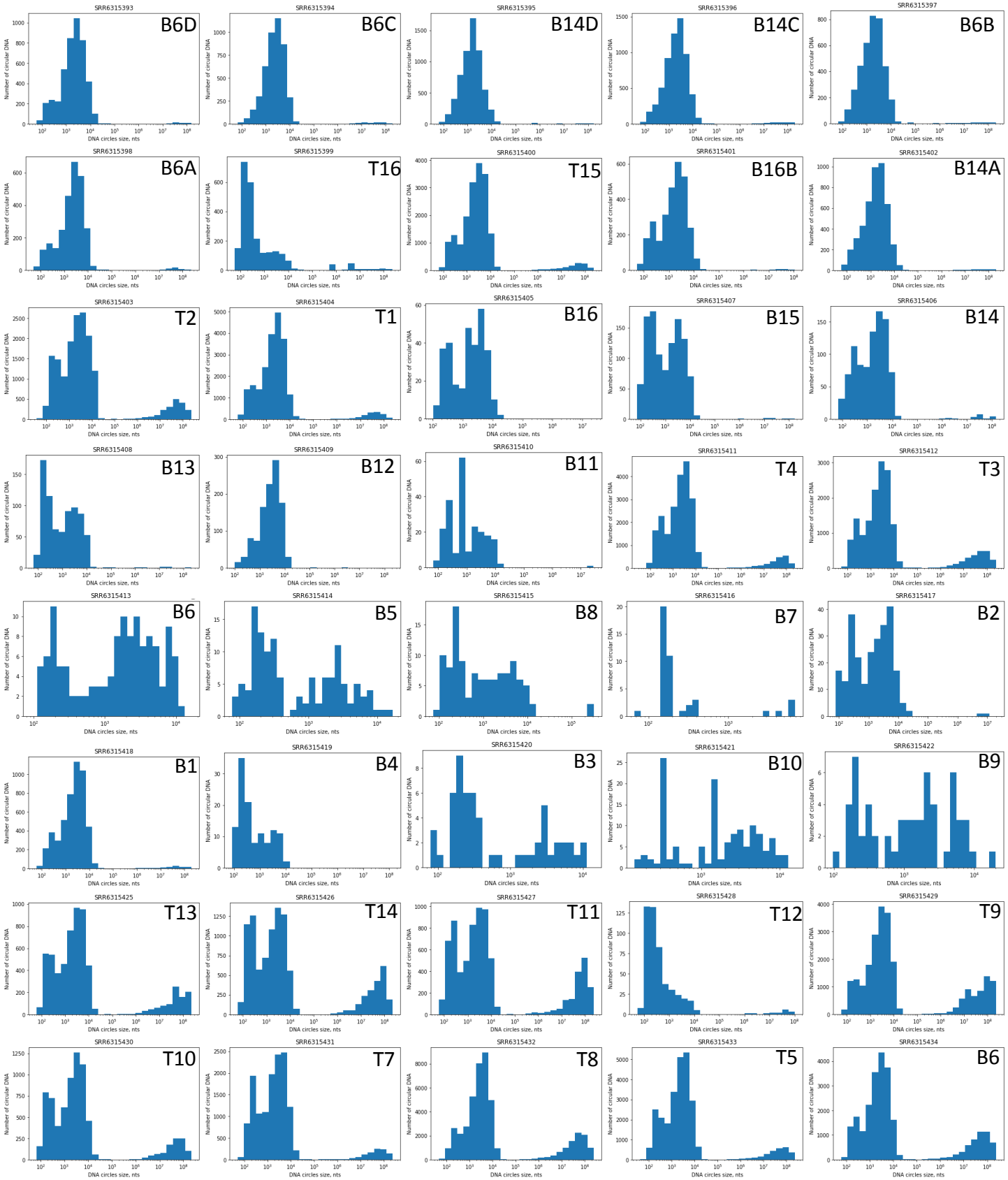

Figure S7. Histograms of the number of eccDNA mapped with Circle_finder (Kumar *et al.*, 2020) using as arguments the hg38 built of the genome and minNonOverlap between two split reads equal to 10. T, SkM tissue sample, B, blood (leukocytes) sample. Odd numbers correspond to sedentary samples; even numbers correspond to active lifestyle samples.